AGU PUBLICATIONS

Geophysical Research Letters

RESEARCH LETTER
10.1002/2015GL066818

Key Points:
- Dense Receiver Functions 3-D seismic imaging of the SW Hellenic subduction
- Slab top segmentation by along-dip faults
- Piecewise roll back induces the Aegean mobility and deformation

Supporting Information:
- Text S1 and Figures S1–S3

Correspondence to:
M. Sachpazi,
m.sachp@noa.gr

Citation:
Sachpazi, M., M. Laigle, M. Charalampakis, J. Diaz, E. Kissling, A. Gesret, A. Becel, E. Flueh, P. Miles, and A. Hirn (2016), Segmented Hellenic slab rollback driving Aegean deformation and seismicity, *Geophys. Res. Lett.*, *43*, 651–658, doi:10.1002/2015GL066818.

Received 30 OCT 2015
Accepted 28 DEC 2015
Accepted article online 30 DEC 2015
Published online 23 JAN 2016

Segmented Hellenic slab rollback driving Aegean deformation and seismicity

M. Sachpazi[1], M. Laigle[2], M. Charalampakis[1], J. Diaz[3], E. Kissling[4], A. Gesret[5], A. Becel[6], E. Flueh[7], P. Miles[8], and A. Hirn[9]

[1]Institute of Geodynamics, National Observatory of Athens, Athens, Greece, [2]Université Nice Sophia Antipolis, CNRS, IRD, Observatoire de la Côte d'Azur, Géoazur UMR 7329, Valbonne, France, [3]Instituto de Ciencias de la Tierra Jaume Almera, ICTJA-CSIC, Barcelona, Spain, [4]Institute of Geophysics, ETH Zurich, Zürich, Switzerland, [5]MINES ParisTech, PSL Research University, Centre de Geosciences, Fontainebleau, France, [6]Lamont-Doherty Earth Observatory, Columbia University, New York, New York, USA, [7]GEOMAR Helmholtz Centre for Ocean Research, Kiel, Kiel, Germany, [8]Commission for the Geological Map of the World, Paris, France, [9]Institut de Physique du Globe de Paris, Sorbonne Paris Cité, Université Paris Diderot, UMR 7154 CNRS, Paris, France

Abstract The NE dipping slab of the Hellenic subduction is imaged in unprecedented detail using teleseismic receiver function analysis on a dense 2-D seismic array. Mapping of slab geometry for over 300 km along strike and down to 100 km depth reveals a segmentation into dipping panels by along-dip faults. Resolved intermediate-depth seismicity commonly attributed to dehydration embrittlement is shown to be clustered along these faults. Large earthquakes occurrence within the upper and lower plate and at the interplate megathrust boundary show a striking correlation with the slab faults suggesting high mechanical coupling between the two plates. Our results imply that the general slab rollback occurs here in a differential piecewise manner imposing its specific stress and deformation pattern onto the overriding Aegean plate.

1. Introduction

Various earlier tectonic models have been proposed to explain the large variations in convergence rate and overriding plate deformation along the western Hellenic subduction zone. These generally appeal to the westward extrusion of Anatolia driven by the collision of Arabia [*McKenzie*, 1972] and the southwestward pull exerted by slab rollback [*Royden*, 1993] (Figure 1 inset). The importance of rapid trench retreat along southern Greece has been shown through GPS studies by the higher southward velocity of the Aegean domain compared to eastern Anatolia [*McClusky et al*., 2000; *Kahle et al*., 2000].

The lack of continuity of North Anatolian Fault through central Greece and the Gulf of Corinth (GoC), both regions of extensional active tectonics [*Goldsworthy et al*., 2002], to the Cephalonia Transform Fault (CTF) and Ionian subduction system leave the debate open between recent conceptual geodynamical models (e.g., slab retreat [*Royden and Papanikolaou*, 2011], slab tearing [*Wortel and Spakman*, 2000; *Govers and Wortel*, 2005; *Jolivet et al*., 2013], and mantle flow [*Faccenna et al*., 2014]).

The large scale structure of the Hellenic subduction has been provided by teleseismic and regional earthquake body wave time delay tomography [*Spakman et al*., 1993; *Papazachos and Nolet*, 1997]. However, important structural details in the upper 100 km layers (e.g., slab topography) could not be resolved. Furthermore, location of intermediate-depth earthquakes in earlier catalogs provides only a crude shape of the dipping zone, not allowing a precise location of the top of the slab [*Papazachos et al*., 2000]. Other structural studies in the Hellenic region based on receiver functions (RF) image the Moho of the subducting slab either at local scale (Crete island [*Knapmeyer and Harjes*, 2000; *Endrun et al*., 2005; *Li et al*., 2003]) or with a very loose sampling at broad scale [*Sodoudi et al*., 2006]. Using data from a dense profile in central Peloponnesus, *Suckale et al*. [2009] have interpreted a slab crust with a 15–20 km thickness from RF imaging. *Gesret et al*. [2010] resolved instead a much thinner crust (LVL), reaching only 7 km of thickness from multiscale analysis of teleseismic *P* to *S* converted waves at four seismic stations at the east coast of Peloponnesus. The data used by *Suckale et al*. [2009] have been reanalyzed in *Pearce et al*. [2012] in conjunction with the data collected along another profile across northern continental Greece. Their results show the subducting slab crust as a dipping low velocity layer with a thickness of 8 km beneath central Peloponnesus and of 20 km under northern Greece. This large difference has been attributed to difference in nature, continental against oceanic subduction, and related to a more significant slab retreat in the Peloponnesus area. However, the two distinct cross sections of the slab, as they are located 300 km apart do not constrain location and geometry of the along-strike variations.

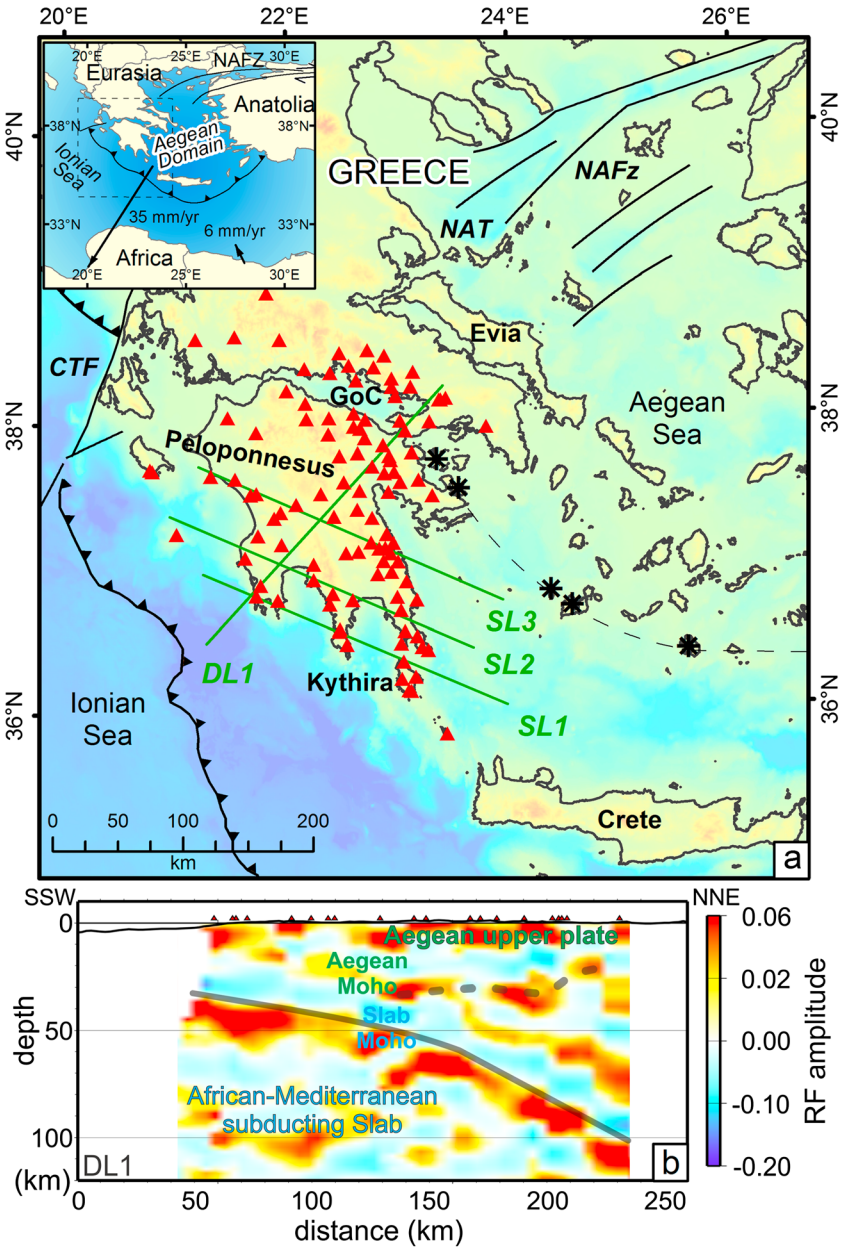

Figure 1. RF imaging along the western Hellenic subduction zone. (a) Main tectonic elements of the study area from W to E: Barbed lines indicate subduction boundaries south and north of Cephalonia Transform Fault (CTF) [*Pearce et al.*, 2012]. Also shown the volcanic Arc [*Nomikou et al.*, 2013] (dashed line) and the North Anatolian Fault Zone (NAFZ) continuation into the Aegean Sea [*Hollenstein et al.*, 2008; *Papanikolaou et al.*, 2002] (black thin lines). Triangles: "TWR" broadband seismic stations. Green lines denote locations of the along-dip and along-strike RF profiles, respectively. GoC: Gulf of Corinth NAT: North Aegean Trough. Inset: Overview with GPS velocity vector for the Aegean plate relative to an Eurasia reference frame [*Kahle et al.*, 2000]. (b) RF profile DL1. Solid grey line: middle of slab crust above red-coded RF amplitude of Moho (see also Figure S3). Dashed grey line: Aegean Moho.

Here we present the results of a 2-D seismic array of ~100 sites we deployed across the whole southern Greece which provide a 3-D image of the topography of the slab. This geometry layout, altogether with the use of high-frequency RF has allowed to improve resolution by over an order of magnitude compared to previous studies, revealing a more complex topography of the slab. Fine relocation of intermediate-depth earthquakes with an improved resolution particularly in depth together with the newly imaged structure allows a joint discussion.

2. Data and Method

In the frame of Thales was right "TWR" European Union (EU) project (2006–2010) a pool of 30–40 three-component broadband stations was deployed from south to central Greece (Figure 1). We have redeployed them several times in different sites in order to improve spatial coverage. Additionally, data from up to 20 permanent broadband stations of the Hellenic National Network located within the studied area as well as a few stations of the NSF funded Multi-disciplinary Experiment for Dynamic Understanding of Subduction under the Aegean Sea (MEDUSA) project have been gathered to complete the TWR data set. This unprecedented dense 2-D array provided a more than 300 km long and 250 km wide coverage of the western part of the Hellenic subduction zone. We analyzed 120 teleseismic events of epicentral distances ranging from 30 to 90° and magnitudes $>$6.0 (Figure S1 in the supporting information). This provided a mean of 30 good quality data per station.

Our study is based on the well-known Ps receiver functions (RFs) technique, which isolates shear (*S*) waves converted from teleseismic compressional (P) waves at lithospheric interfaces of significant velocity contrast such as the crust-mantle boundary (Moho) (Figure S2). A standard receiver function, RF, processing has been applied to the three-component seismograms [e.g., *Langston*, 1977; *Stammler*, 1993; *Kind et al*., 1995]. The Ps (radial component) receiver function is computed for each earthquake by deconvolution of the vertical component from the radial. This processing removes the earthquake source signature and travel-path effects from the source up to the recording station.

The time delay between the converted *P* to *S* wave (Ps) and the direct P wave depends on the depth of the converting interface, the ray parameter and the velocity structure above it. The receiver function records are stacked and transformed from time to depth using a velocity-depth function, here with the International Association of Seismology and Physics of the Earth's Interior standard model to produce depth sections of Ps converted phases beneath the seismic stations (Figures 1b and 2a). It is commonly used as reference model to migrate receiver functions from the time domain to space [*Li et al*., 2003]. Migration though depends strongly on the ray properties such as its back azimuth and incidence angle which are different of the ones when the interface is horizontal. We hence consider RF conversion in a dipping slab. Earthquakes from different azimuths and epicentral distances allow to assess slab top dip and azimuth under a receiver [*Gesret et al*., 2011] which is taken into account with respect to a horizontal interface to migrate the data to the piercing points and obtain the image of the interfaces at depth (Figure 1b).

Subducting crust is expected to appear as a low velocity layer (LVL) embedded between the upper plate mantle and the slab mantle. This geometry is detected by the RF method as a negative followed by a positive polarity signal corresponding to Ps phases (Figure S2). The negative amplitude, caused by downward decreasing velocity, corresponds to the conversion at the top of the subducting oceanic plate (LVL), while the positive amplitude indicates a velocity increase with depth and corresponds to the conversion at its base (Moho). The time difference between the negative and positive Ps signals on the RF seismograms (blue and red on the RF depth sections) is expected to be proportional to the thickness of the subducting crust (LVL). However, this time difference is sensitive to the signal filtering. *Gesret et al*. [2010] based on a multiscale analysis of real and synthetics RFs showed that the only stable part of the signal which remains insensitive to filtering frequencies is the null amplitude between these opposite polarities Ps phases (Figure S3). In the presented depth sections we applied a low frequency filtering to increase the signal to noise ratio. Therefore, for the slab topographic mapping, we picked the transition from the blue to the red band on the RF depth sections (grey lines in Figures 1b and 2a) which marks the middle of the oceanic crust, with the slab Moho and slab top being 3–4 km below and above it, respectively [*Gesret et al*., 2010].

3. Results and Discussion

3.1. Imaging Hellenic Slab Segmentation

We display an example of a vertical section of depth-migrated RF amplitudes in the along-dip direction from SSW to NNE of Peloponnesus (Figure 1b). Below the first clear positive conversion interface located at 25–30 km depth, the upper plate Moho (grey dashed line), a deeper pronounced dipping positive converter between 30 and 100 km depth is imaged. This corresponds to the Moho of the subducting plate, steepening beneath east Peloponnesus at about 60–70 km depth. On the along-strike (WNW-ESE) sections shown in Figure 2a the slab Moho is also clearly imaged as a strong marker horizon. The most striking feature though

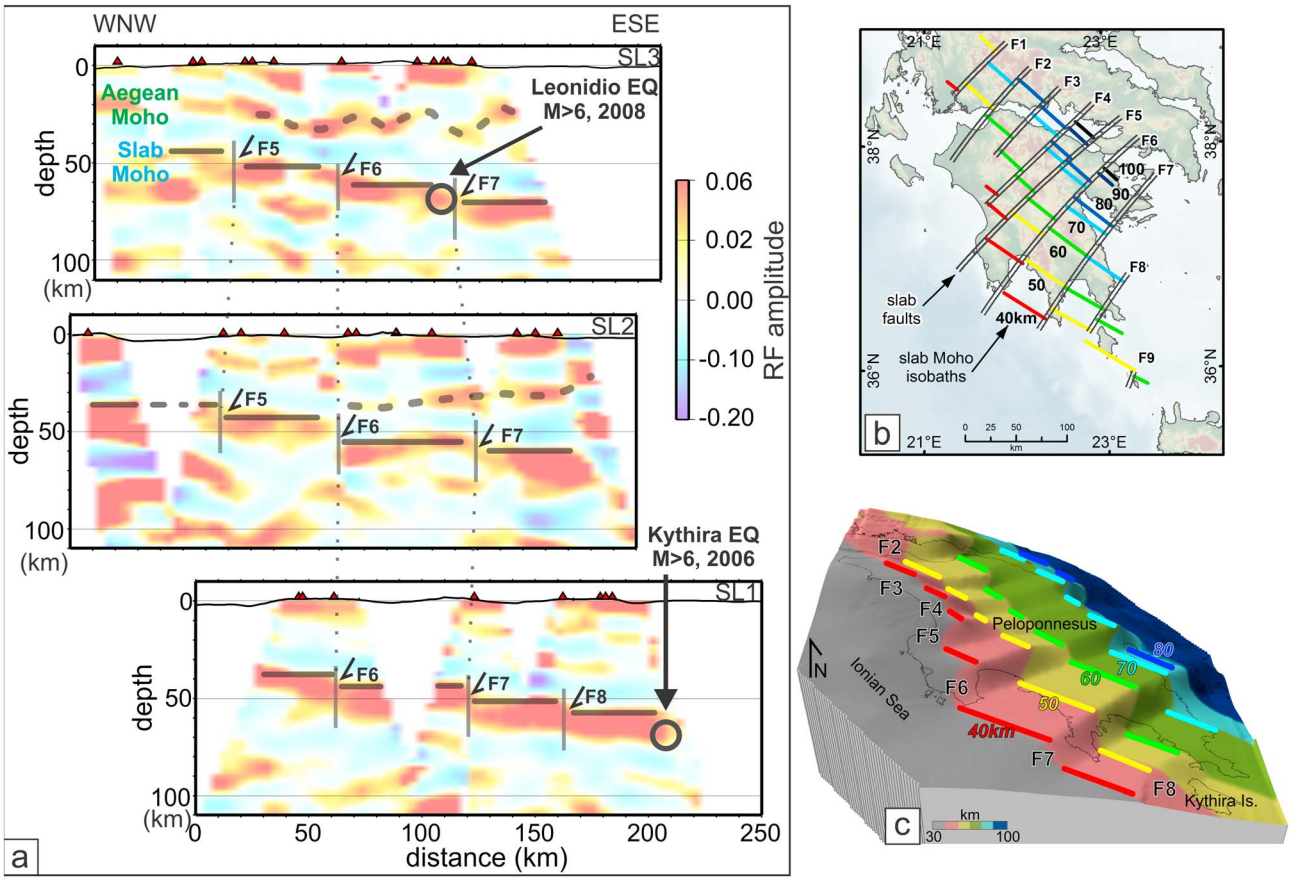

Figure 2. RF-imaging of the structure of the SW Hellenic subduction zone. (a) Along-strike RF sections SL1 to SL3 (locations shown in Figure 1) showing the dipping Hellenic slab panels. Solid grey line: middle of slab crust above red-coded RF amplitude of Moho. Dashed grey line: Aegean Moho. Open circles are hypocenters of slab earthquakes each at a definite throw (half arrow) of the imaged faults. (b) Slab Moho topography and Faults (double lines) mapping reveals an along-dip trend. (c) Perspective view from south of the 3-D topography of slab Moho. Depth color-coded isobaths and shaded fault scarps.

revealed by our data is the appearance of the slab Moho not as a continuous interface but in a fragmented form. Several adjacent subhorizontal segments can be recognized as ESE-ward downstepping panels separated by fault throws of several kilometers. This observation can be made on each of the strike lines and the throws can be correlated from one line to the other as the slab gets deeper, revealing all faults to trend along dip (Figure 2b). Our RF data coverage allows contouring of the slab Moho topography down to 100 km depth to produce a high-resolution 3-D image of the most recently subducted part of the Ionian Sea of the African plate (Figure 2c). It appears segmented from the Gulf of Corinth to south of Kythira island, over 300 km distance, into dipping panels 30–50 km wide by a series of nine along-dip faults (F1 to F9).

3.2. Origin of Slab Faults and Dehydration Processes

In the deep Ionian Abyssal Plain WSW of its lithosphere entering the subduction zone, marine seismic data [*Gallais et al.*, 2011] identify NE-SW oriented faults, interpreted as related to Mesozoic Ionian Sea spreading [*Gallais et al.*, 2011; *Speranza et al.*, 2012]. The faults we image as segmenting downdip the slab top of the same subducted plate show a similarity in orientation that may suggest an inheritance of former structure.

These along-dip faults are marked at depths of 60–80 km by spatial clustering of current small to moderate earthquakes mainly within the slab crust. This seismic activity has been recorded by the TWR dense deployment and the recently improved National Observatory of Athens (NOA) permanent monitoring array (Figure 3a and Text S1). Among mechanisms causing seismic rupture at higher *P-T* conditions than for "normal" frictional conditions in rock, dehydration has been commonly considered as the main responsible for slab earthquakes [*Abers et al.*, 2013]. Interestingly, our observations show that slab top

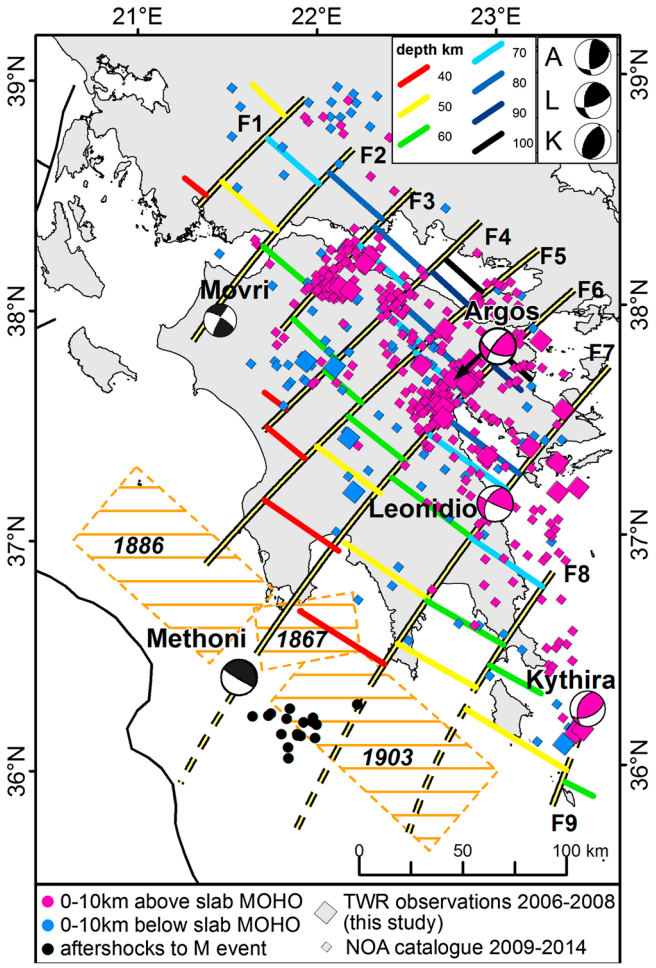

Figure 3. Relation of seismicity with the slab faults in the study area. Slab top seismicity, 10 km below the slab Moho (blue diamonds) and above it (pink diamonds). Note in 60–80 km depths small to moderate magnitude clustering in the vicinity of the faults in the slab crust. The major shallow interplate thrust Mw 6.8 (*M*) Methoni 2008 and main aftershocks (solid black circles) show rupture of whole panel width limited by southwestward prolongation of faults F6 and F7. Focal mechanisms for Argos, Leonidio, and Kythira events are displayed as lower hemisphere projections on the horizontal plane at surface and also on top of the dipping slab (Inset A, L, and K, respectively). Note that when projected onto the dipping slab top the focal mechanisms display essentially reverse slip consistent with the sense of the mapped slab top throws with the strike-slip subdued and they are representative of the real motion of rupture. Also shown the focal mechanism (Centroid Moment Tensor (CMT) Harvard) of the 2008 Movri Mw 6.4 upper plate earthquake. The presumed rupture areas of large megathrust earthquakes in the region are marked by orange. Their magnitudes have been revised from 8.4 and 7.6 [*Wyss and Baer*, 1981] to smaller values of 6.8 and 6.7 [*Papadopoulos*, 2011].

earthquakes occur preferentially at the imaged faults that may have been sites of previous hydratation when it was at sea-bottom.

3.3. Piecewise Slab Roll Back Control on Aegean Deformation

In 2008 two intermediate-depth earthquakes occurred below eastern Peloponnesus with epicenters located 50 km apart (Mw 6.4 6 January at Leonidio and Mw 5.0 18 June at Argos, Figure 3). Historically, no slab earthquakes have occurred on this part of the descending slab and these earthquakes may be considered as the first instrumentally documented events. Observations from the TWR network constrain their hypocenters at 70 km depth within the crust of the slab (Figure 3 and Text S1). Their locations correlate with the positions of the two neighboring faults, F7 and F6 of the slab. A larger slab event (Mw 6.7 Kythira) occurred 2 years earlier and is also coincident with one of the proposed faults (F9) confirming that the RF-imaged faults are seismically active. The focal solutions of the three events show a NE trending nodal plane, which is parallel to the strike of the faults and may thus be considered as the likely fault plane. Their mechanisms projected onto the slab top (Figure 3 inset and Text S1) display reverse slip along these fault planes, consistent with the sense of the mapped slab top throws and a deepening and retreat of the southeastern panel. We hence interpret these earthquakes to be associated with the slab segmentation, illustrating the ongoing slab deformation, caused by the differential vertical motion between the panels, accompanied by a slight component of under thrusting of each panel by its deeper neighbor. Such a mechanism implies that the general slab rollback is occurring in a differential piecewise manner increasing from NNW to SSE (Figure 4). This in turn may induce the fast motion of the Aegean overriding plate toward the SSW which is increasing from NNW to SSE as documented by GPS measurements [*Floyd et al.*, 2010; *Chousianitis et al.*, 2013].

3.4. Along-Strike Segmentation Control on the Size of the Megathrust Earthquakes

Greek historical records include the occurrence of large ($M \geq 8.0$) earthquakes [*Wyss and Baer*, 1981] but their precise location and size are poorly known. Evidence comes from the Methoni (Mw 6.8 14 February 2008)

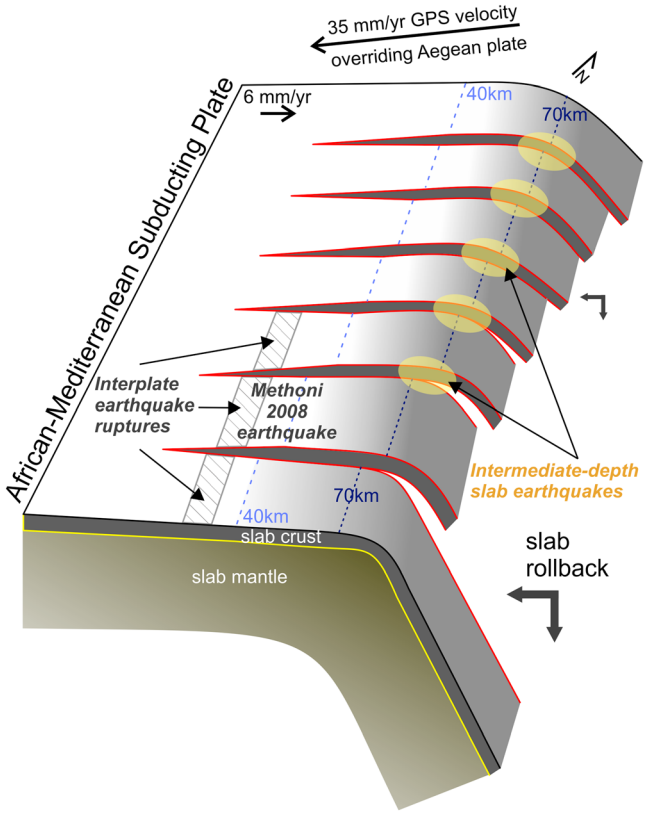

Figure 4. Schematic view from the SE toward NW, with suggested interpretation of features revealed by the 3-D topography of slab structure and seismicity. Yellow ellipses highlight large intermediate-depth earthquakes occurrence as well as clustering of small to moderate earthquakes. Note that slab panel's downdip end is for the sketch purpose and does not mean that they do end at those depths. Dashed black lines indicate the 40 km and 70 km isobaths of the slab Moho. The differential motion between the panels projected on a plane normal to the slab results in a retreat of the ESE, deeper slab panels toward SSW and downward consistently to the general direction of the subduction rollback (thick double arrow).

shallow subduction interplate thrust event which occurred offshore the prolongation of F6 fault (Figure 3 and Text S1). Its main aftershocks delineate a rupture zone which is coincident with the slab panel width to fault F7 imaged onshore. The offshore prolongation of the faults F6 and F7 could have controlled the along-strike limits of the rupture not only of the 2008 Methoni event but also of the large earthquake reported in 1867 (Figure 3) [*Wyss and Baer*, 1981]. Similarly the offshore continuation of faults F5 and F9 could have provided the other side limits to the rupture zones of the 1886 and 1903 interplate earthquakes which occurred on either side of the 2008 event [*Wyss and Baer*, 1981]. The magnitudes of those events have been revised downward from values of ~8.0, [*Wyss and Baer*, 1981] to ~7.0 [*Papazachos and Papazachou*, 2003; *Papadopoulos*, 2011; *Papadopoulos et al.*, 2014]. The rupture lengths associated with those revised magnitudes would thus be closer to the corresponding panel widths. Hence, the slab segmentation appears to control the location and size of major interplate megathrust earthquakes.

3.5. Hypothesis of Mechanical Coupling Between the Two Plates

The Leonidio slab event and the Methoni subduction interplate event are part of a sequence of large earthquakes which stroke the SW Hellenic subduction in the first half of 2008. They have been followed by a NNE right-lateral upper plate event (Achaia-Movri Mw 6.4 8 June 2008) in NW Peloponnesus (Figure 3). *Durand et al.* [2014] suggested a mechanical interaction between the lower and upper plate to explain this 2008 earthquakes sequence. Here we may provide structural elements for a link in space in addition to time. Taking into consideration the observed slab segmentation, these events could be seen as snapshots of a dynamic process involving interplate coupling between the downstepping of the slab panels and the overriding Aegean upper plate. The intermediate-depth events (i.e., Kythira, Leonidio, and Argos events) corresponding to the release of the locally accumulated strain at the slab faults would reflect the retreat of the deeper panels toward the SSW. The Achaia-Movri strike-slip event located uncommonly in the lower than upper Aegean crust right above one of the slab faults (F2) has been attributed to differential shear slip on the base of the Aegean crust [*Serpetzidaki et al.*, 2014]. This specific earthquake may highlight the accommodation of the slab deformation by the overriding upper plate. In the case of interplate coupling, stress will also be increased across the interplate boundary, which can eventually be released by slip over an adjacent panel and thus generating shallow subduction megathrust earthquakes (i.e., Methoni interplate event). Therefore, the 2008 sequence may illustrate the large scale continuous interaction between the two plates. Such a model would explain the relationship between relatively distant events which cannot be understood using simple Coulomb stress.

4. Conclusions

Here we use P to S converted teleseismic waves observed on a dense and expanded seismological network. We resolve fine-scale slab topography which is a drastic revision to the commonly considered smooth shape of the SW Hellenic slab. This high-resolution 3-D image documents the subducting slab as segmented down to 100 km depth by along dip faults. We have resolved intermediate-depth $M > 6$ earthquakes to be located on those faults, which implies that they are seismically active at 70 km depth. We have also constrained the smaller magnitude earthquakes of the slab uppermost part commonly related to dehydration processes to be also clustered along these faults. We further show that the slab faults may control location and size of major historical and instrumental megathrust earthquakes.

Our study provides new and important observations to suggest an unsuspected piecewise, differential roll-back mechanism by a series of at least nine active faults in the SW Hellenic subduction zone. Just above one of the along-dip slab faults we imaged, the Movri right-lateral strike-slip event ruptured the lower crust and Moho of the upper plate, an unprecedented occurrence. Neither surface geology nor the record of former earthquakes had anticipated NE-striking shear zones within the uppermost mantle beneath Peloponnesus. Then, this unexpected occurrence could as well be taken as an indication that other slab faults might also be accompanied above them by similar right-lateral deformation in the upper plate but remained undetectable in the absence of similar significant deep strike-slip earthquake or of surface geology evidences. Such a process above the slab faults distributed over a large region may thus contribute to a transfer of strike-slip motion from where the North Anatolian Fault branches are seen at the surface, to the subduction zone. Our observations may thus provide hints to understand the causes of the mobility and complex deformation of the Aegean upper plate.

Acknowledgments

This research has been supported by the European Union FP6 NEST-INSIGHT program, under project THALES WAS RIGHT and grants from France Germany, Greece, Italy, Spain, and Switzerland to support the huge deployment in the field of instruments of the national and institutional pools. We thank the National Observatory of Athens, NOA for providing data from permanent seismological stations, and MIT for allowing access to Medusa data. We thank the Editor of the journal, an anonymous reviewer and Laurent Jolivet for their critical and constructive suggestions.

References

Abers, G. A., J. Nakajima, P. van Keken, S. Kita, and R. B. Hacker (2013), Thermal-petrological controls on the location of earthquakes within subducting plates, *Earth Planet. Sci. Lett.*, *369*, 178–187.

Chousianitis, K., A. Ganas, and M. Gianniou (2013), Kinematic interpretation of present-day crustal deformation in central Greece from continuous GPS measurements, *J. Geodyn.*, *71*, 1–13.

Durand, V., M. Bouchon, M. A. Floyd, N. Theodulidis, D. Marsan, H. Karabulut, and J. Schmittbuhl (2014), Observation of the spread of slow deformation in Greece following the breakup of the slab, *Geophys. Res. Lett.*, *41*, 7129–7134, doi:10.1002/2014GL061408.

Endrun, B., L. Ceranna, T. Meier, M. Bohnhoff, and H. P. Harjes (2005), Modeling the influence of Moho topography on receiver functions: A case study from the central Hellenic subduction zone, *Geophys. Res. Lett.*, *32*, L12311, doi:10.1029/2005GL023066.

Faccenna, C., et al. (2014), Mantle dynamics in the Mediterranean, *Rev. Geophys.*, *52*, 283–332, doi:10.1002/2013RG000444.

Floyd, M. A., et al. (2010), A new velocity field for Greece: Implications for the kinematics and dynamics of the Aegean, *J. Geophys. Res.*, *115*, B10403, doi:10.1029/2009JB007040.

Gallais, F., M. A. Gutscher, D. Graindorge, N. Chamot-Rooke, and A. D. Klaeschen (2011), Miocene tectonic inversion in the Ionian Sea (central Mediterranean): Evidence from multichannel seismic data, *J. Geophys. Res.*, *116*, B12108, doi:10.1029/2011JB008505.

Gesret, A., M. Laigle, J. Diaz, M. Sachpazi, and A. Hirn (2010), The oceanic nature of the African slab subducted under Peloponnesus: Thin-layer resolution from multiscale analysis of teleseismic *P* to *S* converted waves, *Geophys. J. Int.*, *183*, 833–849, doi:10.1111/j.1365-246X.2010.04738.x.

Gesret, A., M. Laigle, J. Diaz, M. Sachpazi, M. Charalampakis, and A. Hirn (2011), Slab top dips resolved by teleseismic converted waves in the Hellenic subduction zone, *Geophys. Res. Lett.*, *38*, L20304, doi:10.1029/2011GL048996.

Goldsworthy, M., J. Jackson, and J. Haines (2002), The continuity of active fault systems in Greece, *Geophys. J. Int.*, *148*(3), 596–618.

Govers, R., and M. J. R. Wortel (2005), Lithosphere tearing at STEP faults: Response to edges of subduction zones, *Earth Planet. Sci. Lett.*, *236*, 505–523.

Hollenstein, C., M. D. Muller, A. Geiger, and H. G. Kahle (2008), Crustal motion and deformation in Greece from a decade of GPS measurements 1993–2003, *Tectonophysics*, *449*, 17–40.

Jolivet, L., et al. (2013), Aegean tectonics: Strain localisation, slab tearing and trench retreat, *Tectonophysics*, *1*, 597–598.

Kahle, H. G., M. Cocard, Y. Peter, A. Geiger, R. Reilinger, A. Barka, and G. Veis (2000), GPS-derived strain rate field within the boundary zones of the Eurasian, African, and Arabian plates, *J. Geophys. Res.*, *105*, 23,353–23,370, doi:10.1029/2000JB900238.

Kind, R., G. L. Kosarev, and N. V. Petersen (1995), Receiver-functions at the stations of the German Regional Seismic network (GRSN), *Geophys. J. Int.*, *121*, 191–202, doi:10.1111/j.1365-246X.1995.tb03520.x.

Knapmeyer, M., and H. P. Harjes (2000), Imaging crustal discontinuities and the downgoing slab beneath western Crete, *Geophys. J. Int*, *143*, 1–21.

Langston, A. C. (1977), The effect of planar dipping structure on source and receiver responses for constant ray parameter, *Bull. Seismol. Soc. Am.*, *67*, 1029–1050.

Li, X., G. Bock, A. Vafidis, R. Kind, H. P. Harjes, W. Hanka, K. Wylegalla, M. Van Der Meijde, and X. Yuan (2003), Receiver function study of the Hellenic subduction zone: Imaging crustal thickness variations and the oceanic Moho of the descending African lithosphere, *Geophys. J. Int.*, *155*, 733–748, doi:10.1046/j.1365-246X.2003.02100.x.

McClusky, S., et al. (2000), Global Positioning System constraints on plate kinematics and dynamics in the eastern Mediterranean and Caucasus, *J. Geophys. Res.*, *105*, 5695–5719, doi:10.1029/1999JB900351.

McKenzie, D. (1972), Active tectonics of the Mediterranean region, *Geophys. J. R. Astr. Soc.*, *30*(2), 109–185.

Nomikou, P., D. Papanikolaou, M. Alexandri, D. Sakellariou, and G. Rousakis (2013), Submarine volcanoes along the Aegean volcanic arc, *Tectonophysics*, *597*, 123–146.

Papadopoulos, G. A. (2011), *A Seismic History of Crete: The Hellenic Arc and Trench, Earthquake and Tsunamis 2000 BC–2011 AD*, Ocelotos Publ. Sci., Athens.

Papadopoulos, G. A., I. Baskoutas, and A. Fokaefs (2014), Historical seismicity of the Kyparissiakos Gulf, western Peloponnese Greece, *B. Geofis. Teor. Appl.*, *55*, 389–404.

Papanikolaou, D., M. Alexandri, P. Nomikou, and D. Ballas (2002), Morphotectonic structure of the western part of the North Aegean Basin based on swath bathymetry, *Mar. Geol.*, *190*, 465–492.

Papazachos, B. C., and K. Papazachou (2003), *The Earthquakes of Greece*, 286 pp. (in Greek), Ziti Publ, Thessaloniki.

Papazachos, B. C., V. G. Karakostas, C. B. Papazachos, and E. M. Scordilis (2000), The geometry of the Wadati-Benioff zone and lithospheric kinematics in the Hellenic arc, *Tectonophysics*, *319*, 275–230.

Papazachos, C., and G. Nolet (1997), P and S deep velocity structure of the Hellenic area obtained by robust nonlinear inversion of travel times, *J. Geophys. Res.*, *102*, 8349–8367, doi:10.1029/96JB03730.

Pearce, F. D., S. Rondenay, M. Sachpazi, M. Charalampakis, and L. H. Royden (2012), Seismic investigation of the transition from continental to oceanic subduction along the western Hellenic Subduction Zone, *J. Geophys. Res.*, *117*, B07306, doi:10.1029/2011JB009023.

Royden, L. H. (1993), The tectonic expression of slab pull at continental convergent boundaries, *Tectonics*, *12*, 303–325, doi:10.1029/92TC02248.

Royden, L. H., and D. J. Papanikolaou (2011), Slab segmentation and late Cenozoic disruption of the Hellenic arc, *Geochem. Geophys. Geosyst.*, *12*, Q03010, doi:10.1029/2010GC003280.

Serpetzidaki, A., P. Elias, M. Ilieva, P. Bernard, P. Briole, A. Deschamps, S. Lambotte, H. Lyon-Caen, E. Sokos, and G. A. Tselentis (2014), New constraints from seismology and geodesy on theMw = 6.4 2008 Movri (Greece) earthquake: Evidence for a growing strike-slip fault system, *Geophys. J. Int.*, *198*, 1373–1386.

Sodoudi, S., R. Kind, D. Hatzfeld, K. Priestley, W. Hanka, K. Wylegalla, G. Stavrakakis, A. Vafidis, H. P. Harjes, and M. Bohnhoff (2006), Lithospheric structure of the Aegean obtained from P and S receiver functions, *J. Geophys. Res.*, *111*, B12307, doi:10.1029/2005JB003932.

Spakman, W., S. Van Der Lee, and R. Van Der Hilst (1993), Travel-time tomography of the European-Mediterranean mantle down to 1400 km, *Phys. Earth Planet. Int.*, *79*, 3–74.

Speranza, F., L. Minelli, A. Pagnatelli, and M. Chiappini (2012), The Ionian Sea: The oldest in situ ocean fragment of the world?, *J. Geophys. Res.*, *117*, B12101, doi:10.1029/2012JB009475.

Stammler, K. (1993), Seismic handler—Programmable multichannel data handler for interactive and automatic processing of seismological analyses, *Comput. Geosci.*, *19*, 135–140, doi:10.1016/0098-3004(93)90110-Q.

Suckale, J., S. Rondenay, M. Sachpazi, M. Charalampakis, A. Hosa, and L. H. Royden (2009), High-resolution seismic imaging of the western Hellenic subduction zone using teleseismic scattered waves, *Geophys. J. Int.*, *178*, 775–791, doi:10.1111/j.1365-246X.2009.04170.x.465.

Wortel, M. J. R., and W. Spakman (2000), Subduction and slab detachment in the Mediterranean-Carpathian region, *Science*, *290*, 1910–1917, doi:10.1126/science.290.5498.1910.

Wyss, M., and M. Baer (1981), Earthquake hazard in the Hellenic arc, in *Earthquake Prediction: An International Review*, vol. 4, edited by D. W. Simpson and P. G. Richards, pp. 153–172, AGU Maurice Ewing Ser., Washington, D. C.